Influence of Morphology on the Transport Properties of Perfluorosulfonate Ionomers/Polypyrrole Composite Membrane

HoSeok Park,[†] YoJin Kim,[†] Won Hi Hong,*[,†] Yeong Suk Choi,[‡] and HongKee Lee[§]

Department of Chemical and Biomolecular Engineering, KAIST, 373-1 Guseong-dong, Yusong-gu, Daejeon, Republic of Korea; Fuel Cell Program Team, SAIT (Samsung Advanced Institute of Technology), San14-1, Nongseo-Ri, Kihueng-Eup, Yongin-Shi, Kyunggi-Do, Republic of Korea; and Korea Institute of Industrial Technology 472, Kajwa 4-dong, Seo-Ku, Incheon, 404-254, Republic of Korea

Received November 15, 2004; Revised Manuscript Received December 30, 2004

ABSTRACT: Nanosized polypyrrole particles were mainly incorporated into the ionic clusters rather than the nonpolar backbone of Nafion in chemical in-situ polymerization by means of ion−dipole interaction between the sulfonate groups of Nafion and secondary amonium groups of polypyrrole. The incorporation of polypyrrole particles into the clusters, where was the transport pathway, could change the morphology of Nafion matrix, as observed by DSC, SAXS, and WAXD. In particular, the crystallite region of backbones as well as the cluster region of side chains was influenced indirectly by the existence of polypyrrole particles in the ionic clusters. Additionally, the temperature of the cluster transition shifted to a higher value due to the restricted mobility of the clusters, whereas the melting temperature of the nonpolar backbone crystallite shifted to a lower value due to the disruptive effect of swelled cluster. The methanol crossover was reduced more than the proton conductivity because of the existence of polypyrrole particles in the ionic clusters. Suggestions were made as to how the polypyrrole particles existed in the matrix of Nafion and how they influenced the transport properties of composite membranes.

Introduction

Nafion, which is a commercially representative perfluorosulfonate ionomer, can conduct cations, such as proton, with good chemical and thermal stability.[1] This material can be applied to a variety of electrochemical processes and devices, and it is especially used as the polymer electrolyte of a direct methanol fuel cell (DMFC). However, the methanol crossover by electroosmotic drag and diffusion decreases the performance of the cell by mixed potential.[2] A number of different approaches extensively mitigate the effects of the methanol crossover in a DMFC. These approaches mainly consist of changing operational parameters such as the flow rate, fuel concentration, pressure at the cathode, and temperature as well as developing or modifying the material. Many researches have studied the polymer electrolyte membrane (PEM) because of intrinsic limitations that result from controlling the operating conditions in a DMFC, and they highlighted the perfluorosulfonate ionomer/conducting polymer composite membranes.[3,4]

Perfluorosulfonate ionomer/conducting polymer composites have extraordinary properties. For example, they combine the high cationic conductivity of the perfluorosulfonate ionomer with the electrocatalytic activity of the conducting polymer.[4] In the case of polypyrrole, the electrocatalytic activity may cause methanol oxidation.[26] These composites have been investigated extensively because of their characteristics. In one study, the composite membranes of Nafion and polypyrrole were prepared by the electrodeposition of polypyrrole on a Nafion-coated electrode.[5] Pickup and co-workers investigated the polymerization mechanism of pyrrole in the Nafion matrix and the enhancement of the performance in a DMFC.[3,4] A novel method of deposing thin Pt catalysts on Nafion membranes impregnated with polypyrrole was proposed for unitized regenerative fuel cells (URFCs).[6]

Despite this interest, few studies have been undertaken on the morphology of these composite membranes with a conducting polymer in the field of fuel cells. Therefore, attention should be given to investigation into the change of ionomeric structure in the Nafion matrix after chemical in-situ polymerization of pyrrole monomers due to the effects of morphology on the transport phenomenon in the membrane. Research has examined how the transport properties of methanol can be influenced by the change of morphology.

Experimental Section

Materials. Nafion 115 membrane for this experiment, which was supplied by E.I. Dupont de Nemours & Co., had an equivalent weight of 1100 g for each sulfonic acid. Pyrrole was purchased from Sigma Aldrich and used as received. Extra-pure hydrogen peroxide (35 wt %) was purchased from Junsei Chemical and used as an oxidant for polymerization.

Preparation of Nafion. Nafion membranes were purified by first heating themselves in high-purity water containing 3 wt % H_2O_2 for 1 h at about 70−80 °C and repeated the process four times in high-purity water to completely remove all traces of H_2O_2. A similar heating treatment was used in H_2SO_4 1 M for 1 h, and the treatment was repeated several times in high-purity water to remove the sulfuric acid.

Preparation of the Composite Membrane. After drying pretreated Nafion membranes at room temperature under vacuum for 24 h, they were immersed for 5 min in an aqueous pyrrole solution whose concentration ranged from 0.03 to 1 M. To in-situ polymerize the pyrrole monomers in an aqueous solution, they were immersed in 30 wt % H_2O_2 for 5 min. After the in-situ polymerization, the modified membranes were posttreated in order to remove the unreacted pyrrole monomers. All samples were treated with nitric acid and sulfuric acid to change all the composite membranes into an H form. A 1 N sodium hydroxide solution was used to change some of

[†] KAIST.
[‡] SAIT.
[§] Korea Institute of Industrial Technology 472.
* Corresponding author: e-mail whhong@kaist.ac.kr.

10.1021/ma047650y CCC: $30.25
Published on Web 02/16/2005

the unmodified Nafion-H membranes into a Na form to compare Nafion-H with Nafion-Na.[7] The composite membranes are notated as N/P 001 at 0.06 M, N/P 002 at 0.2 M, and N/P 003 at 0.6 M pyrrole solution.

The procedures to prepare the dried or rehydrated samples before any characterization step are as follows:

All samples were dried under vacuum at room temperature for 24 h. However, they were in the partially drying state because the samples contained residual water.[9,11] Residual water was measured by TGA analysis. Nafion had a mass loss of 3.15%, which was almost attributed to water loss. N/P 001 and N/P 003 decreased 2.48 and 0.92 wt %, respectively. The dried samples were carefully sealed to prevent additional water absorption before any measurement in the drying state.

To prepare the rehydrated samples, the predried samples were immersed in the deionized water for 7 days and kept in the sealed Petri dish full of the deionized water. Because the humidity of atmosphere during any measurement was below 100% and the level of hydration was reduced, the rehydrated samples were in the partially hydrating state. As soon as taking out the sample from the deionized water, all measurements were immediately carried out to maintain the levels of hydration.

Instrumental Methods. SEM images were obtained by a field emission scanning electron microscope (Philips SEM 535M) equipped with a Schottky-based field emission gun. TEM images were collected on an E.M. 912Ω energy-filtering transmission electron microscope (EF TEM) with bright filtered imaging (120 kV). The EF TEM, which is installed at Korea Basic Science Institute, is from Carl Zeiss, Germany.

To measure dense polymer film, FT-IR ATR spectra were collected on a JASCO FT-IR 470 plus as attenuated total reflection. Each spectrum, which was recorded as the average of 48 scans with a resolution of 4 cm^{-1}, was collected from 4000 to 650 cm^{-1}. The pressure was equal in all samples to avoid differences caused by the pressure and penetrating depth.

Differential scanning calorimetry (DSC, DuPont TA 2000) calibrated with indium was used to study the thermal behavior of the Nafion and the composite membranes. Each sample was loaded in hermetically sealed aluminum pans and scanned at a heating rate of 10 °C/min within 30−300 °C under a nitrogen atmosphere.

With a counting time of 2 h, small-angle X-ray scattering (SAXS) data were gathered on a Rigaku D/max-2500 (5 kW) with an image plate system equipped with a Cu Kα radiation generator. Wide-angle X-ray diffraction (WAXD) data were obtained on a Rigaku D/max lllC (3 kW) with θ/θ goniometer equipped with Cu Kα radiation generator. The diffraction angle of the diffractograms was in the range of $2\theta = 10-25°$.

The proton conductivity of membranes was measured by the ac impedance spectroscopy over a frequency range of 10^{-3}−10^{6} Hz with 10 mV. A system based on a Solatron 1255 frequency response analyzer was used to measure the proton conductivity of membranes with a two-point probe cell. The conductivity of the sample was obtained from complex impedance analysis. The real and imaginary parts of the complex impedance were plotted, and the proton conductivity was obtained from the bulk resistance found in complex impedance diagram. The proton conductivity can be calculated by using the equation $\sigma = L/RA$, where L and A are the thickness of the sample and the surface area of the electrode and R is the resistance from the impedance data.

As a result of the concentration gradient, the methanol passed through the electrolyte membrane into the opposite cell. To determine the degree to which the membrane had been permeated, the permeability of methanol for Nafion and composite membranes was measured. The device depicted in Scheme 1 was used to measure the permeation. A refractometer (ATAGO 3T) was used to measure the concentration of the methanol.

Scheme 1. Schematic Diagram of the Cell for the Methanol Crossover Measurement

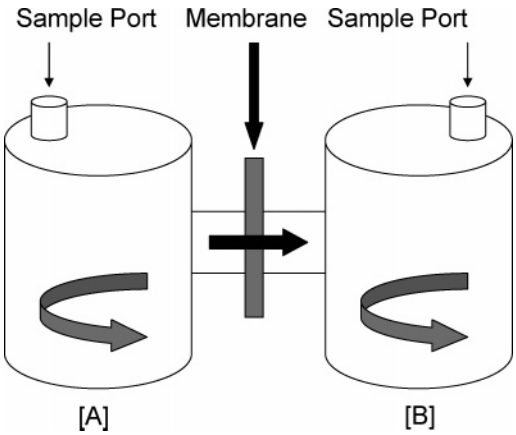

Results and Discussion

Polypyrrole identification. Figure 1 shows how the polypyrrole contents increase as a function of pyrrole concentration at room temperature. At first, the polypyrrole contents increased rapidly. As the concentration of the pyrrole monomers gradually increased, the polypyrrole contents almost reached a constant value above 0.6 M of the pyrrole solution. This behavior was attributed to the limitation of ionic sites of Nafion. To analyze how the polypyrrole particles influence the morphology, unsaturated N/P 001 and peudo-saturated N/P 003 were chosen as representatives.

The SEM images in Figure 2A,B show the inside of the Nafion and the composite membrane N/P 001. No pores were detected in either membrane, and both membranes had dense structures. Further, the presence of typical polypyrrole particles was clearly observed as white spots. TEM images were used to confirm the existence and size of the polypyrrole particles in the Nafion matrix, the results of which are shown in Figure 3A,B. The white spots were caused by the grid. In line with the SEM results, the TEM images show nanosized polypyrrole particles with black spots at about 20−40 nm. A comparison of parts A and B of Figure 3 shows the dependence of the increased polypyrrole contents on the pyrrole concentration.

State of the Polypyrrole Particle in Nafion Matrix. FT-IR measurements were carried out to investigate the state of polypyrrole in the Nafion matrix. Bands at about 1400 and 910 cm^{-1} are assigned as S=O and S−OH stretching bands of sulfonic group which is an association form.[10] To investigate whether secondary ammonium groups of polypyrrole could be ion-

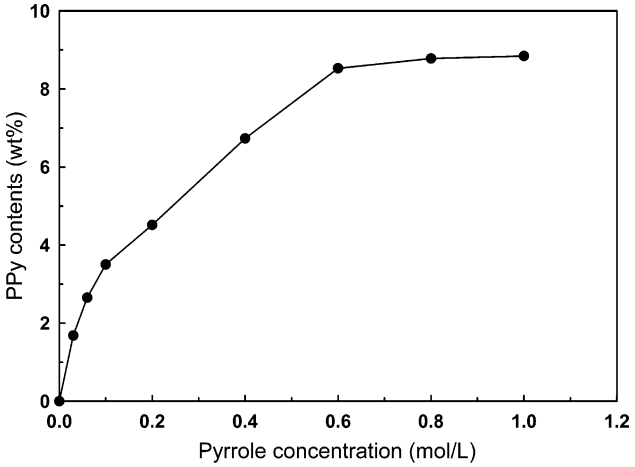

Figure 1. Changes in the polypyrrole content as a function of pyrrole concentration at room temperature.

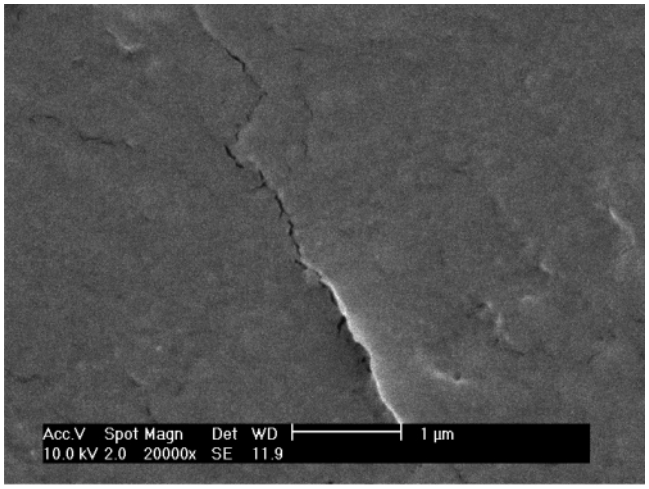

(A)

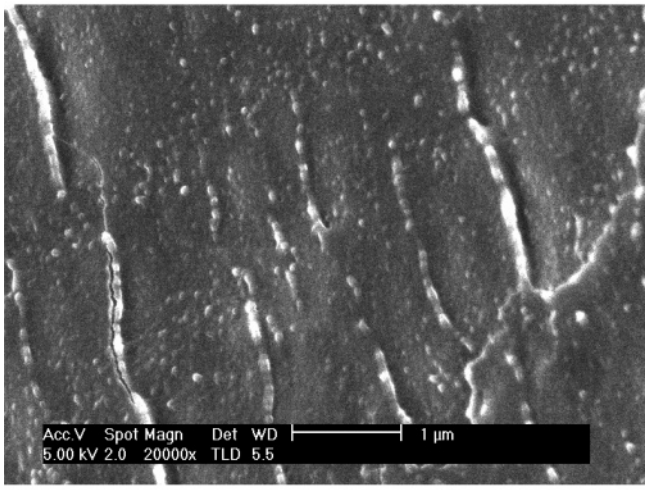

(B)

Figure 2. SEM images of (A) Nafion and (B) N/P 001. All samples were in the partially drying state.

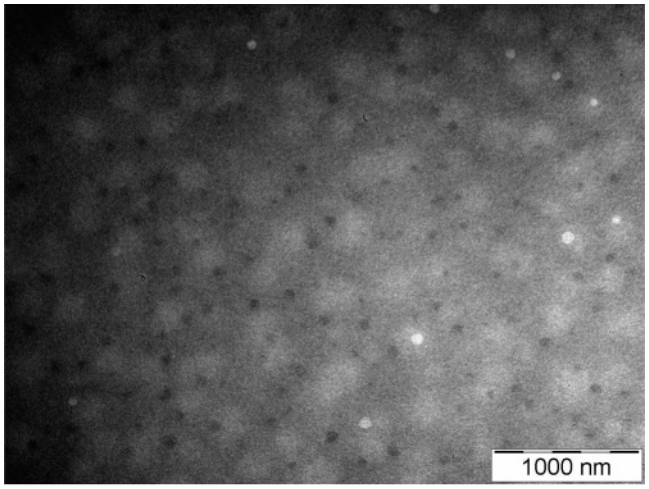

(A)

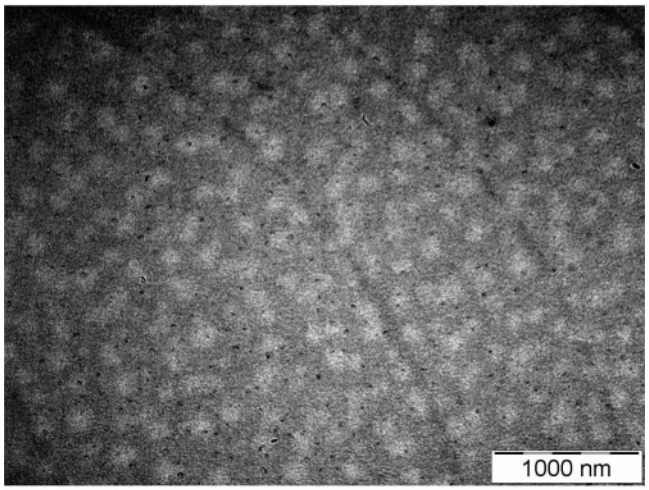

(B)

Figure 3. TEM images of (A) N/P 001 and (B) N/P 003. All samples were in the partially drying state.

exchanged with the protons interacted with sulfonate groups, however, the peak of sulfonate group rather than that of sulfonic group is analyzed. The chemical environment or surroundings influences the spectra. The degree of hydration and the counterion type affect significantly the peaks of sulfonate groups which are dissociation forms of sulfonic groups.[8−10] Unfortunately, the asymmetric SO_3^- stretching vibration bands were masked by the strong C−F stretching vibration bands at about 1200 cm^{-1}.[11] The shifts in the symmetric SO_3^- stretching vibration peaks are due to the polarization of the S−O dipole by the electrostatic field of adjacent counterions.[12] At a high degree of hydration or fully hydration state, the position of peak is independent of the types of counterions because each sulfonate group is shielded from the nearest counterion by several water molecules.[12]

Figure 4 shows the symmetric SO_3^- stretching vibration bands of partially dried Nafion-H, hydrated Nafion-H, dried Nafion-Na, and dried composite membranes at about 1050 cm^{-1}. The positions of the symmetric SO_3^- stretching peaks differed for each membrane. If all the membranes are at a degree of hydration lower than 7 wt % or full drying,[13] the difference in the position of each peak may reflect the ionic strength of the sulfonate

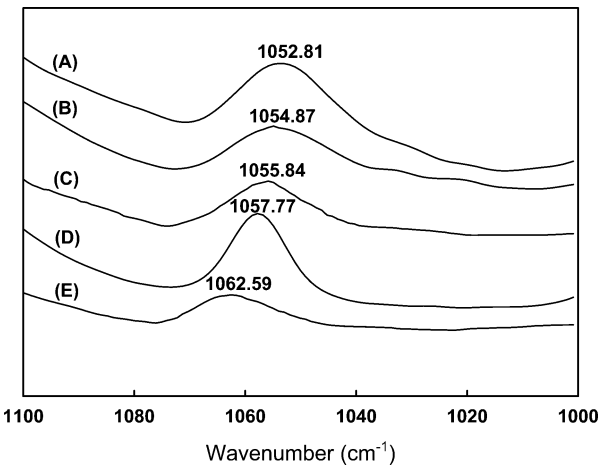

Figure 4. FT-IR ATR spectra of the 1100−1000 cm^{-1} region of (A) dried Nafion-H, (B) dried N/P 001, (C) dried N/P 003, (D) hydrated Nafion-H, and (E) dried Nafion-Na.

groups in the membranes, thereby reflecting the effect of chemical environment or surroundings. When comparing the hydrated Nafion-H with the dried Nafion-H, it is known that the hydrated Nafion-H is almost in a dissociatied form, whereas the dried Nafion-H is

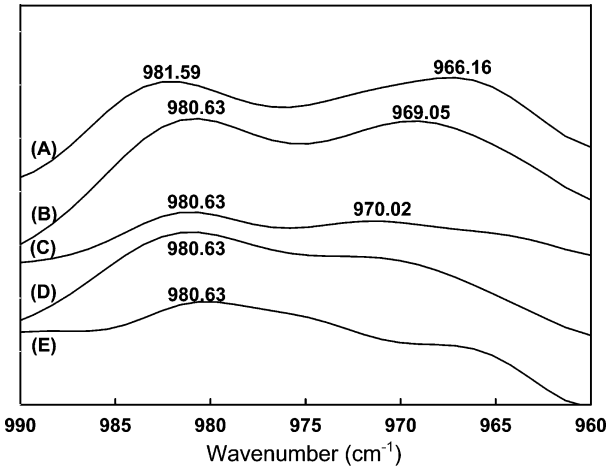

Figure 5. FT-IR ATR spectra of the 990−960 cm^{-1} region of (A) dried Nafion-H, (B) dried N/P 001, (C) dried N/P 003, (D) hydrated Nafion-H, and (E) dried Nafion-Na.

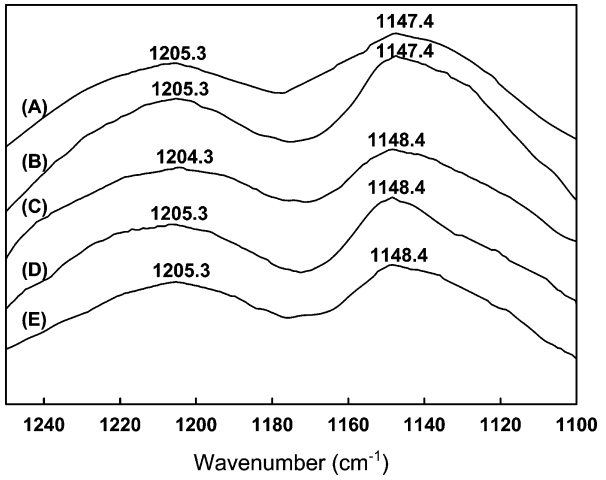

Figure 6. FT-IR ATR spectra of the 1250−1100 cm^{-1} region of (A) dried Nafion-H, (B) dried N/P 001, (C) dried N/P 003, (D) hydrated Nafion-H, and (E) dried Nafion-Na.

almost in an associated form. It is shown in Figure 4A,D that both types of Nafion-H had different peak positions due to the polarization of the S−O dipole that was attributed to the difference in the hydrogen-bonding interaction. The shift of peak as a result of the effect of counterion could also be shown in Figure 4A,E when protons were exchanged with sodium ions, which are metal ions.[13] In the same manner, polypyrrole also existed in cation form in the Nafion matrix due to its basicity and shifted the positions of peaks at about 1050 cm^{-1}, as shown in Figure 4A−C. Although the composite membranes could form hydrogen bonds between the sulfonate groups of Nafion and secondary ammonium groups of polypyrrole, the interactions of the hydrogen bonds differed from the interactions of the hydrated Nafion-H. In most cases, the position of peak can be determined by the following principle: the stronger electrostatic polarization, the higher peak shift.[8] The N/P 003 shifted to higher wavenumbers than the N/P 001. It is expected that the number of polypyrroles, which interacted with ionic sites of Nafion, influenced the electrostatic interaction.

Figure 5 shows the symmetric C−O−C stretching vibration bands at about 980 and 960 cm^{-1}. The positions of these peaks correspond respectively to the C−F stretching ($-CF_2-CF(CF_3)-$ group) peak and the symmetric C−O−C stretching peak. In the same manner as Figure 4, the change in these peak positions depended on a variety of chemical environments. However, as a result of nonpolarity, the C−F stretching peak was hardly influenced by the counterion type. On the other hand, the shift in or even disappearance of the symmetric C−O−C stretching peak depended on the counterion type and the degree of hydration. Lone electrons of oxygen can electrostatically interact with metal ion or form hydrogen bonds with proton.[10] In the case of Nafion-Na and hydrated Nafion-H, the symmetric C−O−C stretching peaks were disappeared. The peaks at 960 cm^{-1} in the composite membrane were shifted. The secondary ammonium ions of polypyrrole were ion-exchanged with protons shielding the sulfonate groups of side chains and interacted with oxygen of the $-CF_2-CF(CF_3)-$ groups.

Figure 6 shows the spectra of the CF_2 group, which represents the backbone. The band at 1205 cm^{-1} is attributed to the asymmetric CF_2 stretching peak, and the band at 1148 cm^{-1} is assigned to the symmetric CF_2 stretching peak.[9] Furthermore, chemical in-situ polymerization of the pyrrole monomers hardly shifted the position of the two peaks because of the noninteraction between the nonpolar backbone and the polar polypyrrole. Therefore, the secondary ammonium groups of polypyrrole particles interacted with the sulfonate groups of the pendant side chain rather than with the backbone.

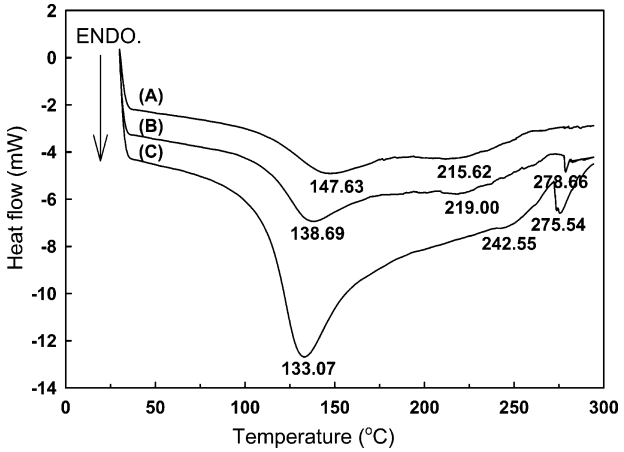

Figure 7. DSC thermograms of (A) N/P 003, (B) N/P 001, and (C) Nafion in the drying state.

Morphology. Two kinds of endothermic peaks can be observed in a typical DSC curve of Nafion. The first endothermic peak, which is interpreted as cluster transition temperature, can be accompanied by a polymer contraction due to the loss of water, with a resulting increase in entropy.[14] This peak shows a strong endothermic peak at about 140 °C. Second, there is a weak and broad endothermic peak at about 250 °C, which is assigned to the melting peak of the nonpolar crystallite backbone.[15]

Figure 7 compares the DSC curves of Nafion and the composite membranes N/P 001 and N/P 003. The incorporation of polypyrrole into the Nafion matrix increased the temperature of the cluster transition and decreased the melting temperature of the nonpolar crystallite. It is assumed that the pyrrole monomers mostly invade the polar clusters rather than the nonpolar backbone because of the polarity of themselves. When the pyrrole concentration increased, more protonated polypyrrole particles were ion-exchanged with the

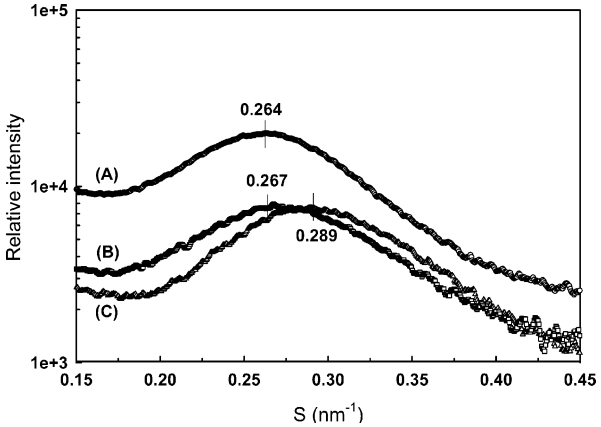

Figure 8. SAXS curves of (A) hydrated Nafion, (B) hydrated N/P 001, and (C) dried Nafion.

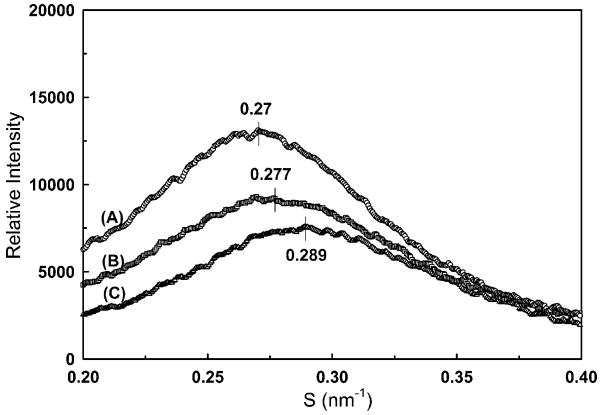

Figure 9. SAXS curves of (A) N/P 003, (B) N/P 001, and (C) Nafion in the drying state.

protons interacted with the sulfonate groups in the cluster due to the increasing polypyrrole contents. The ionic interaction between the secondary ammonium groups of polypyrrole and sulfonate groups of Nafion restricted molecular mobility as a result of the immobilization of the cluster and increased the cluster transition temperature.

The presence of side chains and ionic aggregates, which can disturb the crystallization of the polymer chains, may cause the melting temperature of the nonpolar crystallite backbone to shift at a temperature lower than that observed in the PTFE, which is approximately 320 °C.[16] Therefore, the changes in this peak are strongly related to crystallization. It is supposed that the changes in the ion aggregates or cluster that are caused by incorporation of polypyrrole particles can influence crystallinity or the crystallite size. In addition, Nafion and the composite membrane N/P 001 showed a sharp endothermic peak above 250 °C. This peak may be associated with thermal degradation of side chains, which can be related to SO_2 liberation.[17] The formation of the Nafion$-SO_3^-$ and $^+NH_2-$polypyrrole ionic pair could stabilize the C−S bond because the composite membranes had a higher SO_2 liberation temperature than Nafion. The N/P 003 did not even appear in this range. Thus, the ionic interaction between the sulfonate groups of Nafion and secondary ammonium groups of polypyrrole particles could obstruct the degradation of sulfonate groups.

Figure 8 shows the SAXS curves for the partially dried, hydrated Nafion, and hydrated composite membrane N/P 001. The pyrrole monomer consists of a nonpolar ring and a polar amino group, both of which enable the polypyrrole particles to be incorporated into the nonpolar backbone or polar cluster. By revealing the changes in the clusters of the composite membranes, the SAXS data confirm the existence of polypyrrole particles in the ionic clusters. In this S range, the SAXS peak is attributed to the scattering from the ionic clusters.[18,19] The ionic clusters preferentially take up water by hydrophilicity, thereby increasing the size of ionic cluster and causing the shift in the ionic scattering maximum to approach a smaller S.[20] The dried and hydrated Nafion showed these results clearly. When Nafion absorbed more water, the scattering intensity increased due to the enhancement of the difference in the electron density by decreasing the electron density of the clusters relative to the backbone.[18−20] The position of scattering maximum is inversely proportional to the Bragg spacing. The increase in the Bragg spacing as a result of absorbing water is due either to the increased intercluster distance according to the two-phase model[21] or to the increased short-range order distance according to the core−shell model.[19] This result means that the absorbed water can swell the ionic clusters of the dried Nafion. A comparison Nafion with N/P 001 in the hydrating state shows that Nafion has a larger intensity than the composite membranes due to more water uptake, as shown in Table 2. In the case of the scattering maximum, although N/P 001 had less water uptake than Nafion, both of them almost had similar values. It is supposed that the Bragg spacing was affected by the incorporation of polypyrrole particles as well as the absorption of water.

Table 2. Transport Properties of Nafion and Composite Membranes

	Nafion	N/P 001	N/P 002	N/P 003
water uptake (wt %)	24.5	22.3	16.2	12.5
methanol uptake (wt %)	61.1	55.3	46.3	32.5
relative proton conductivity	1	0.875	0.463	0.033
relative methanol crossover	1	0.570	0.240	0.029

When the dried Nafion was compared with the dried composite membranes N/P 001 and N/P 003, the results differed from those of the hydration state. Figure 9 compares the dried Nafion with the composite membranes. In the drying state of our experimental condition, Nafion contained more residual water than the composite membranes. Thus, the incorporation of polypyrrole into the clusters increased the difference in the electron density between the ionic clusters and the backbone and extended the Bragg spacing as a result of a swelling effect, such as water. The pseudo-saturated composite membrane N/P 003 reached the Bragg spacing of 37 Å and determined the specific size of the ionic clusters. The water content dominantly influenced the scattering intensity in the hydrating state, whereas the

Table 1. SAXS Data of Nafion, N/P 001, and N/P 003 in the Hydrating and Drying State

	Nafion		N/P 001		N/P 003	
	drying state	hydrating state	drying state	hydrating state	drying state	hydrating state
scattering vector (nm^{-1})	0.289	0.264	0.277	0.267	0.270	–
Bragg spacing (Å)	34.6	38	36.2	37.5	37	–

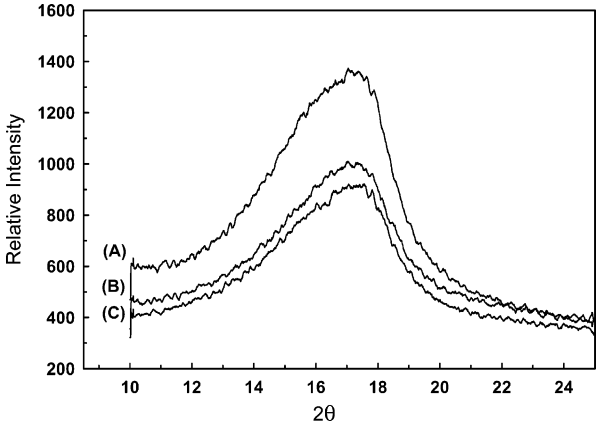

Figure 10. WAXD curves of (A) Nafion, (B) N/P 001, and (C) N/P 003 in the drying state.

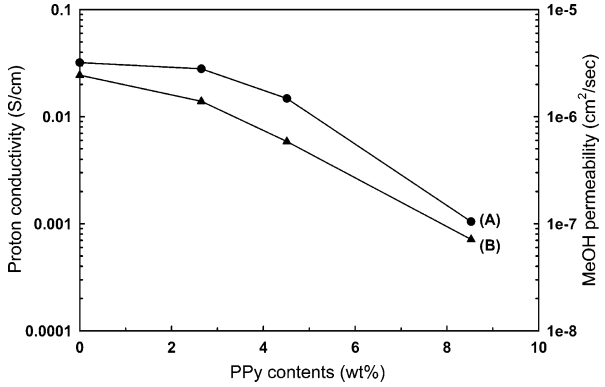

Figure 11. Changes in the (A) proton conductivity and (B) methanol permeability as functions of polypyrrole contents.

polypyrrole particles dominantly influenced the scattering intensity in the drying state. When the polypyrrole particles were present, the polypyrrole contents rather than the water uptake affected the Bragg spacing in the drying state.

As shown in Figure 7, the composite membranes had a lower melting temperature of nonpolar crystallite backbone than Nafion. The WAXD was used to investigate the relation between the melting temperature and the crystallite region. Figure 10 shows typical wide-angle diffractograms. Both Nafion and the composite membranes show a crystalline reflection (indexed as the 100 reflection of the hexagonal structure),[22] and the crystalline reflection is superimposed as a shoulder on a large amorphous halo. Unfortunately, the superposition of the sharp crystalline peak and the broad amorphous halo by the low level of crystallinity in the 1100 EW Nafion[23] made it impossible to separate and qualitatively analyze two peaks. However, the shape of the Nafion is slightly sharper than the shapes of the composite membranes. This broadening effect probably included the effects of lattice distortions and small crystallite size, both of which were caused by the incorporation of polypyrrole into cluster, but it was difficult to separate them because of the low crystallinity.[23] The lower melting temperature of nonpolar crystallite backbone that was caused by an invasion of polypyrrole particles into the clusters was mainly attributed to the disruptive effect of swelled clusters on the lamellar ordering of nonpolar backbone.[24] In general, crystallite plays a role in blocking water sorption. Therefore, the more crystallinities the membrane has, the less water it absorbs.[25] The composite membranes, however, had less water uptake despite having less crystallinities. It is plausible to say that the reduced mobility or dense structure by the ion−dipole interaction in the cluster, which was shown by the increased cluster transition temperature, could hinder the water sorption.

Analysis on the Transport Properties in the Composite Membrane. The cell performance in a DMFC is mainly determined by the proton conductivity and methanol crossover. In general, a good performance needs high proton conductivity and low methanol crossover. In our transport experiment, each sample was measured above five times. Every result was averaged in the error range of ±5%. As shown in Figure 11, when the polypyrrole content increases, the proton conductivity of composite membranes decreases. This phenomenon is due to two factors: first, the decreased mobility of the ionic clusters despite the swell of clusters, as shown in Figure 7; and second, the dense structure by ion−dipole interaction between the polypyrrole and Nafion, as shown by SEM and FT-IR data. The methanol crossover in Figure 11 was also decreased by these effects when the polypyrrole content increased. Table 2 shows that the relative proton conductivity is higher than the relative methanol permeability. Compared to Nafion, the N/P 001 had about 13% less proton conductivity and 43% less methanol permeability. Furthermore, the transport properties of ionomer were dominantly affected by ionic cluster. The methanol crossover was reduced more than the proton conductivity despite the swelling effect of the clusters. This difference in reduction was attributed to the effect of polypyrrole

Scheme 2. Structure of the Nafion/Polypyrrole Composite Membrane

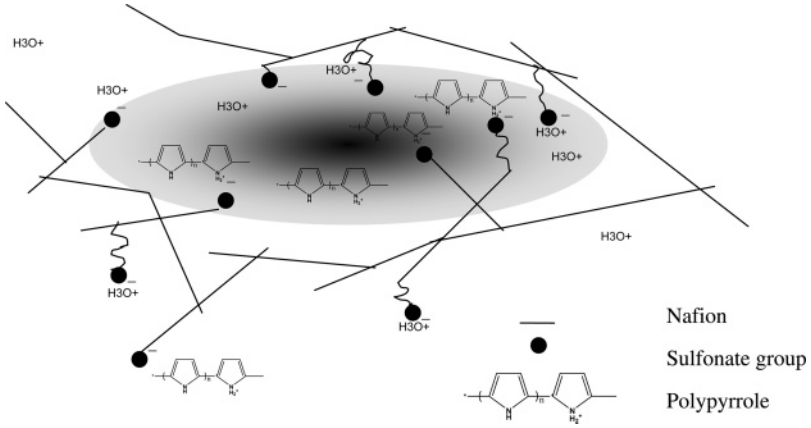

particles in the ionic clusters, where was the transport pathway. It is expected that in an electrochemical environment, or during cell operation, the methanol crossover of the composite membranes will be decreased more without reducing the proton conductivity further. That is due to the occurrence of methanol oxidation by means of the higher electrocatalytic activity of polypyrrole particles.[26] In addition, our group has researched on the optimization of performance in the composite membranes as a function of polypyrrole content.

Conclusions

Using various instruments, it was observed how chemical in-situ polymerization changed the morphology of the Nafion. Scheme 2 shows the morphology of composite membranes. After in-situ polymerization, nanosized polypyrrole particles were distributed in the Nafion matrix at about 20−40 nm. Nonporous and dense structures remained without microphase separation, as shown by the SEM images and DSC curves. These structures were due to the ion−dipole interaction between the sulfonate groups of Nafion and secondary ammonium groups of polypyrrole, as shown by FT-IR data. This interaction between the polypyrrole and Nafion matrix enhanced the cluster transition and SO_2 liberation temperatures of the composite membranes. The incursion of the composite membranes into the clusters swelled the clusters and decreased the electron density of the ionic clusters. In addition, the polypyrrole particles in the ionic clusters influenced the nonpolar crystallite backbone and blocked the crystallization of the backbone, thereby affecting the transport properties. Table 2 shows that the uptakes of water and methanol decrease. In the case of N/P 001, the decrease in the methanol crossover was sharper than the decrease in the proton conductivity. It is deduced that nanosized polypyrrole particles in the cluster, particularly in the pathway of methanol crossover as well as proton conduction, could decrease the methanol crossover, despite the swelling clusters. The content of the incorporated polypyrrole could be responsible for the characteristics of the ionic clusters that affect transport phenomenon.

Acknowledgment. This research was supported by the Brain Korea 21 (BK 21) project and Korea Institute of Industrial Technology. We thank them for funding.

References and Notes

(1) Kim, Y. J.; Choi, W. C.; Woo, S. I.; Hong, W. H. *Electrochim. Acta* **2004**, *49*, 3227−3234.
(2) Jiang, R.; Chu, D. *Electrochem. Solid State Lett.* **2002**, *5*, A156−159.
(3) Easton, E. B.; Langsdorf, B. L.; Hughes, J. A.; Sultan, J.; Qi, Z.; Kaufman, A.; Pickup, P. G. *J. Electrochem. Soc.* **2003**, *150*, C735−C739.
(4) Langsdorf, B. L.; Maclean, B. J.; Halfyard, J. E.; Hughes, J. A.; Pickup, P. G. *J. Phys. Chem. B* **2003**, *107*, 2480−2484.
(5) Chang, C. M.; Huang, H. J. *Anal. Chim. Acta* **1995**, *300*, 15−23.
(6) Lee, H. Y.; Kim, J. Y.; Park, J. H.; Joe, Y. G.; Lee, T. H. *J. Power Sources* **2004**, *131*, 188−193.
(7) Kim, Y. J.; Choi, W. C.; Woo, S. I.; Hong, W. H. *J. Membr. Sci.* **2004**, *238*, 213−222.
(8) Kujawski, W.; Nguyen, Q. T.; Neel, J. *J. Appl. Polym. Sci.* **1992**, *44*, 951−958.
(9) Gruger, A.; Régis, A.; Schmatko, T.; Colomban, P. *Vib. Spectrosc.* **2001**, *26*, 215−225.
(10) Buzzoni, R.; Bordiga, S.; Ricchiardi, G.; Spoto, G.; Zecchina, A. *J. Phys. Chem.* **1995**, *99*, 11937−11951.
(11) Ludvigsson, M.; Lindgren, J.; Tegenfeldt, J. *Electrochim. Acta* **2000**, *45*, 2267−2271.
(12) Lowry, S. R.; Mauritz, K. A. *J. Am. Chem. Soc.* **1980**, *102*, 4665−4667.
(13) Bernson, A.; Lindgren, J. *Solid State Ionics* **1993**, *60*, 37−41.
(14) Lage, L. G.; Delgado, P. G.; Kawano, Y. *Eur. Polym. J.* **2004**, *40*, 1309−1316.
(15) Stefanithis, I. D.; Mauritz, K. A. *Macromolecules* **1990**, *23*, 2397−2402.
(16) Villani, V.; Pucciairello, R.; Ajroldi, G. *J. Polym. Sci., Polm. Phys. Ed.* **1991**, *29*, 1255−1259.
(17) Wilkie, C. A.; Thomsen, J. R.; Mittleman, M. L. *J. Appl. Polym. Sci.* **1991**, *42*, 901−909.
(18) Roche, E. J.; Pineri, M.; Duplessix, R.; Levelut, M. *J. Polym. Sci., Polym. Phys. Ed.* **1981**, *19*, 1−11.
(19) Gierke, T. D.; Munn, G. E.; Wilson, F. C. *J. Polym. Sci., Polym. Phys. Ed.* **1981**, *19*, 1687−1704.
(20) Marx, C. L.; Caufield, D. F.; Cooper, S. L. *Macromolecules* **1973**, *6*, 344−353.
(21) Fujimura, M.; Hashimoto, T.; Kawai, H. *Macromolecules* **1981**, *14*, 1309−1315.
(22) Howard, W.; Starkweater, Jr. *Macromolecules* **1982**, *15*, 320−323.
(23) Debolt, L. C.; Suter, U. W. *Macromolecules* **1987**, *20*, 1425−1428.
(24) Moore, III, B. R.; Martin, C. R. *Macromolecules* **1989**, *22*, 3594−3599.
(25) Lee, C. H.; Hong, W. H. *J. Membr. Sci.* **1997**, 187−193.
(26) Kulesza, P. J.; Matczak, M.; Wolkiewics, A.; et al. *Electrochim. Acta* **1999**, *44*, 2131−2137.

MA047650Y